Deficit in knee extension strength following anterior cruciate ligament reconstruction is explained by a reduced neural drive to the vasti muscles

Nuccio, Stefano; Vecchio, Alessandro Del; Casolo, Andrea; Labanca, Luciana; Rocchi, Jacopo Emanuele; Felici, Francesco; Macaluso, Andrea; Mariani, Pier Paolo; Falla, Deborah; Farina, Dario; Sbriccoli, Paola

DOI:
10.1113/JP282014

Deficit in knee extension strength following anterior cruciate ligament reconstruction is explained by a reduced neural drive to the vasti muscles

Stefano Nuccio[1], Alessandro Del Vecchio[2], Andrea Casolo[3], Luciana Labanca[1], Jacopo Emanuele Rocchi[4], Francesco Felici[1], Andrea Macaluso[1,4], Pier Paolo Mariani[4], Deborah Falla[5], Dario Farina[6], Paola Sbriccoli[1]

Affiliations:

[1] Department of Movement, Human and Health Sciences, University of Rome "Foro Italico", Rome, Italy

[2] Department Artificial Intelligence in Biomedical Engineering, Friedrich-Alexander University, Erlangen-Nürnberg, 91052, Erlangen, Germany.

[3] Department of Biomedical Sciences, University of Padova, Padua, Italy

[4] Villa Stuart Sport Clinic-FIFA Medical Centre of Excellence, Rome, Italy

[5] Centre of Precision Rehabilitation for Spinal Pain (CPR Spine), School of Sport, Exercise and Rehabilitation Sciences, University of Birmingham, Birmingham, UK.

[6] Department of Bioengineering, Imperial College London, London, UK

Corresponding author:

Prof. Paola Sbriccoli, MD, Ph.D

Department of Movement, Human and Health Sciences University of Rome "Foro Italico"; Piazza Lauro de Bosis 6, Rome, Italy, I- 00135; Phone/Fax. +39 06 376733 214; e-mail: paola.sbriccoli@uniroma4.it

KEY POINTS

- Impaired expression and control of knee extension forces are common after anterior cruciate ligament reconstruction and are related to a high risk of a second injury.
- To provide novel insights into the neural basis of this impairment, we investigated the discharge patterns of motor units in the vastus lateralis and vastus medialis during voluntary force contractions.
- We found a lower knee extensor's strength of the reconstructed side with respect to the contralateral side, which was explained by deficits in motor unit discharge rate and an altered motoneuronal input-output gain. Insufficient excitatory inputs to motoneurons and increased inhibitory afferent signals potentially contributed to these alterations.
- These results further our understanding of the neural underpinnings of quadriceps weakness following anterior cruciate ligament reconstruction and can help to develop effective rehabilitation protocols to regain muscle strength and reduce the risk of a second injury.

ABSTRACT

The persistence of quadriceps weakness represents a major concern following anterior cruciate ligament reconstruction (ACLR). The underlying adaptations occurring in the activity of spinal motoneurons are still unexplored. This study examined the discharge patterns of large populations of motor units (MUs) in the vastus lateralis (VL) and vastus medialis (VM) muscles following ACLR.

Nine ACLR individuals and ten controls performed unilateral trapezoidal contractions of the knee extensor muscles at 35%, 50% and 70% of the maximal voluntary isometric force (MVIF). High-density surface electromyography (HDsEMG) was used to record the myoelectrical activity of the *vasti* muscles in both limbs. HDsEMG signals were decomposed with a convolutive blind source separation method and MU properties were extracted and compared between sides and groups.

The ACLR group showed a lower MVIF on the reconstructed side compared to the contralateral side (28.1%; P<0.001). This force deficit was accompanied by reduced MU discharge rates (~21%; *P*<0.05), lower absolute MU recruitment and derecruitment thresholds (~22% and ~22.5%, respectively; *P*<0.05) and lower input-output gain of motoneurons (27.3%; *P*=0.009). Deficits in MU discharge rates of the VL and in absolute recruitment and derecruitment thresholds of both *vasti* MUs were associated with deficits in MVIF (*P*<0.05). A strong between-side correlation was found for MU discharge rates of the VL of ACLR individuals (P<0.01). There were no significant between-group differences (P>0.05).

These results indicate that mid-to-long term strength deficits following ACLR may be attributable to a reduced neural drive to *vasti* muscles, with potential changes in excitatory and inhibitory synaptic inputs.

Keywords: ACL reconstruction; neural impairment; discharge rate; high-density electromyography; quadriceps weakness; motor unit

INTRODUCTION

Anterior cruciate ligament reconstruction (ACLR) is the most widely adopted procedure to allow ACL injured athletes to resume their pre-injury level of sport participation. Nevertheless, as a direct consequence of ACLR, the majority of patients develop a substantial neuromuscular impairment of the quadriceps, known as arthrogenic muscle inhibition (AMI) (Rice & McNair, 2010). AMI is markedly high during the first months after surgery and tends to progressively decrease across the rehabilitation process (Palmieri-Smith *et al.*, 2008). However, insufficient quadriceps strength and activation may also persist even years after ACLR (Ingersoll *et al.*, 2008). For instance, one study reported that 80% of fully rehabilitated ACLR elite soccer players failed to achieve satisfactory quadriceps strength symmetry (limb symmetry index ≥ 90%) upon return to sport (~8 months after surgery) (Herrington *et al.*, 2018). Persistently weak knee extensors may lead to long-term functional impairments (Palmieri-Smith & Lepley, 2015), early development of knee osteoarthritis (Palmieri-Smith *et al.*, 2009) and increased risk of second ACL injuries, particularly within the first months after return to sport (Grindem *et al.*, 2016; Kyritsis *et al.*, 2016).

An impaired spinal reflex excitability has been documented acutely after ACLR (Lepley *et al.*, 2015) and therefore linked to AMI and to its causal factors, such as pain, swelling and mechanoreceptor disruption (Rice & McNair, 2010). By contrast, mid-to-long term deficits in quadriceps strength and function have been related to an impaired excitability of cortical descending pathways (Kuenze *et al.*, 2015; Palmieri-Smith & Lepley, 2015). Furthermore, indirect evidence of neuroplasticity has been recently provided by Grooms and colleagues (2017) who reported greater activation of brain areas responsible for motor planning and attention in ACLR patients than controls. Although these previous studies have provided some insights into the spinal and supraspinal mechanisms underlying the persistence of quadriceps weakness (PQW), how these alterations affect the motor output delivered by spinal motoneurons to the muscle is still largely unknown, as potential changes in motor unit activity have been only hypothesised (Konishi *et al.*, 2002; Bryant *et al.*, 2008) or indirectly inferred (Nuccio *et al.*, 2020).

The recent development of decomposition techniques for the identification of motor unit discharge timings from high-density surface electromyography (HDsEMG) (Del Vecchio *et al.*, 2020), has allowed to accurately study the adaptations of large populations of motor units (MUs) in response to different stimuli, such as training (Del Vecchio *et al.*, 2019; Casolo *et al.*, 2020) and pathological conditions (Castronovo *et al.*, 2017). This study was designed to examine the discharge patterns of *vasti* MUs following ACLR. Due to the well-established ACLR-related impairment in the voluntary activation of the knee extensor muscles (Hart *et al.*, 2010; Kuenze *et al.*, 2015; Lepley *et al.*, 2015), we hypothesised that the reconstructed side would show a lower force and substantial alterations in MU activity compared to both the contralateral side and a control group.

METHODS

Participants

Nineteen male soccer players volunteered to participate in this cross-sectional study (**Table 1**). Ten out of nineteen underwent ACLR within the previous twelve months. Enrolled ACLR soccer players were operated by the same orthopaedic surgeon (PP.M.) within thirty days from their ACL injury, using either an ipsilateral bone-patellar tendon-bone (BPTB) or a semitendinosus-gracilis tendon (STGR) autograft and followed the same standardized rehabilitation program (Labanca *et al.*, 2018; Rocchi *et al.*, 2018). Nine healthy soccer players, who were matched by physical activity level (Tegner & Lysholm, 1985), were included as controls. Previous history of knee or quadriceps injury, anterior knee pain during open kinetic chain exercises and a Tegner score < 7 were adopted as exclusion criteria. Informed written consent was signed by all participants and the experimental protocols and procedures were approved by the Internal Review Board of the University of Rome “Foro Italico” and conformed to the standards set by the Declaration of Helsinki.

Table 1. *Participant demographics*

Characteristics	Group		P value
	ACLR *(n=10)*	**CONTROL** *(n=9)*	
Age (y)	24.8 ± 3.2	25.7 ± 2.5	.52
BMI ($kg \cdot m^{-2}$)	23.3 ± 0.6	22.9 ± 0.5	.14
Tegnere Activity Level score (range: 1-10)	7.6 ± 1.0	7.9 ± 1.1	.56
sCKRS score (range: 0-100)	92.6 ± 2.7	100 ± 0	< 0.001 *
Graft	BPTB (n=8/10) STGR (n=2/10)	NA	NA
Concomitant Injuries	No other injuries (n=8/10) Meniscus medialis (n=2/10)	NA	NA
Time after ACL surgery (days)	244.4 ± 84.5	NA	NA

*BMI = Body Mass Index; sCKRS= Modified Subjective Cinccinati Knee Rating Scale; BPTB=Bone-Patellar Tendon-Bone graft; * significantly different*

Overview

Participants visited the laboratory on two different occasions. During the first visit they familiarized with the experimental procedures by performing a series of maximal and submaximal isometric voluntary knee extensions. Subjective scores of knee function were collected during this session, using the modified version of the Cincinnati Knee Rating Scale questionnaire (CKRS) (Shelbourne & Nitz, 1992). In the second visit, which was held twenty-four hours after the familiarization session, participants underwent the main experimental session, which involved the simultaneous recordings of voluntary isometric knee extensor force (during maximal and submaximal contractions) and HDsEMG signals from both vastus lateralis (VL) and vastus medialis (VM) muscles.

Experimental Protocol

After a standardized warm-up (Nuccio *et al.*, 2020), participants performed 3-4 trials (~ lasting 3-5 s each) during which they were verbally encouraged to reach their unilateral maximal voluntary isometric force (MVIF) by pushing “as hard as possible”. Rest between trials was ~ 60 s. Approximately 5 minutes after, they were instructed to

perform submaximal trapezoidal contractions at three different force targets (2 X 35, 50, 70 %MVIF), characterized by a recruitment (linear increase in force at 5% MVIF·s^{-1}), a plateau (10 s of constant force at target), and a derecruitment (linear decrease in force at 5% MVIF·s^{-1}) phase. Participants were asked to exert force with their knee extensors and match as accurately as possible a visual template of the trapezoidal path, which was displayed on a monitor placed 1 m away from the participants. Three-minutes of rest were provided between all submaximal contractions. All measurements were performed bilaterally and both the first side to be tested and the first trapezoidal contraction to be performed, were randomly determined. Participants were asked to avoid strenuous exercise and caffeine intake in the 48 hours preceding the test.

Force and HDsEMG recordings

Force and HDsEMG signal recordings followed the same procedures described in detail elsewhere (Nuccio *et al.*, 2020). Briefly, participants were comfortably seated and fastened to a Kin-Com dynamometer (KinCom, Denver, USA) by means of three different Velcro straps (thigh, chest, pelvis), with the knee joint fixed at 45° of flexion (full knee extension at 0°)(**Figure 1A**). Two bi-dimensional grids of 64 electrodes each (5 columns X 13 rows; gold-coated; diameter of 1 mm; inter-electrode distance of 8 mm; OT Biolettronica, Turin, Italy) were used to record HDsEMG signals from the *vasti* muscles (**Figure 1B**). The optimal orientation and positioning of the electrode grids over VL and VM surfaces were determined in accordance with existing guidelines (Barbero *et al.*, 2012) and adjusted following the same procedures as in our previous investigation (Nuccio *et al.*, 2020). After skin shaving and cleansing (70% ethanol), both electrode grids were attached to muscle surfaces using two disposable bi-adhesive foam layers (SpesMedica, Battapaglia, Italy). Skin-electrode contact was ensured by filling the foam layer holes with conductive paste (SpesMedica, Battapaglia, Italy). A ground electrode was placed on the contralateral wrist, whereas reference electrodes for both VL and VM grids were placed on the ipsilateral patella and medial malleolus, respectively. The monopolar HDsEMG signals were recorded using a multichannel amplifier (EMG-Quattrocento, A/D converted on 16 bits; bandwidth 10–500 Hz; OT Biolelettronica, Turin, Italy), amplified (X 150) and band-pass filtered (10-500 Hz) at source, prior to offline analysis. Force and HDsEMG signals were sampled at 2048 Hz

and collected simultaneously using the software OTBioLab (OTBioelettronica, Turin, Italy). Both force templates and real-time biofeedback of the exerted force were displayed at a uniform visual gain during each trial through a custom LabVIEW software (LabVIEW 8.0; National Instruments).

Data Analysis

Force signal analysis

The force signal was converted to Newtons (N) and low-pass filtered with a cut-off frequency of 15 Hz (4^{th} order, zero-lag, Butterworth filter). A gravity correction was applied to remove the signal offset. The trapezoidal contractions characterized by evident pre-activations ($\leq$ 0.5 N from the baseline force signal in the 150 ms prior to the force onset) or countermovement were discarded.

Motor unit analysis

In offline analyses, monopolar HDsEMG signals were band-pass filtered (20-500 Hz) using a 2^{nd} order Butterworth filter. A validated convolutive blind source separation technique (Holobar & Zazula, 2007; Holobar *et al.*, 2014) was adopted to decompose the HDsEMG signal into individual MU discharge timings, which were subsequently converted into binary spike-trains. Identified spike-trains were then manually inspected by an experienced operator and those showing poor signal quality were removed (Holobar & Zazula, 2007). Specifically, MUs showing a pulse-to-noise ratio (PNR) $\leq$ 30 dB (decomposition accuracy $\leq$ 90%) and/or an inter-spike time interval higher than 2s were excluded from further analysis (Holobar *et al.*, 2014). Raster plots in **Figure 1C-D-E-F** show the spike trains of MUs identified during different trapezoidal contractions. For each example pool of MUs, the cumulative spike train (CST) was computed (Thompson *et al*., 2018; Del Vecchio *et al.*, 2018), low-pass filtered using a 4^{th} order 10 Hz Butterworth filter and superimposed to raster plots. The high similarity between Force and CST traces suggests that the smoothed CST (i.e., indicative of the effective neural drive to the muscle) provides a good estimation of muscle force generation.

MU recruitment threshold (RT) and de-recruitment threshold (DERT) were defined as the absolute (N) and relative (%MVIF) force levels at which each MU discharged its first and last action potential, respectively. Mean MU discharge rate (DR) was calculated for each phase and throughout the entire trapezoidal contraction. Specifically, MU DR at recruitment and de-recruitment were calculated from the first four and the last four discharge timings, whilst DR at plateau was computed from the discharge timings identified during the whole plateau phase. For each participant, values of MU RT, DERT and DR extracted from trials at similar relative force levels were firstly averaged (e.g., over the 2 x 50% MVIF). Then, to examine the adaptations of *vasti* MUs, the resulting participant-specific values were averaged across target forces (35-50-70 %MVIF) within each lower limb and muscle. The relative contribution of low- and high-threshold MUs (LTMUs, HTMUs) to side-to-side differences in MU DR was additionally examined in the ACLR group, by arbitrarily clustering MUs according to their RT (LTMUs: ≤ 30% MVIF; HTMUs: > 30% MVIF). To perform this analysis, the activity of MUs identified within the same lower limb and muscle was averaged across target forces, for each participant. The relationship between the change in discharge rate (ΔDR_{R-T}) from recruitment (mean DR of the first 4 MU action potentials) to target force (mean DR of the whole plateau phase) relative to the change in force ($\Delta Force_{R-T}$) from recruitment (force at which MUs were recruited) to target (force at 35, 50, 70 %MVIF), was examined at subject-specific level in both absolute (N) and relative (%MVIF) values to estimate the input-output relationship of the quadriceps motoneuron pool. This analysis provides indirect information on the synaptic input received by the motoneuron pool, representing the sum of all the inputs converging from the different levels of the nervous system.

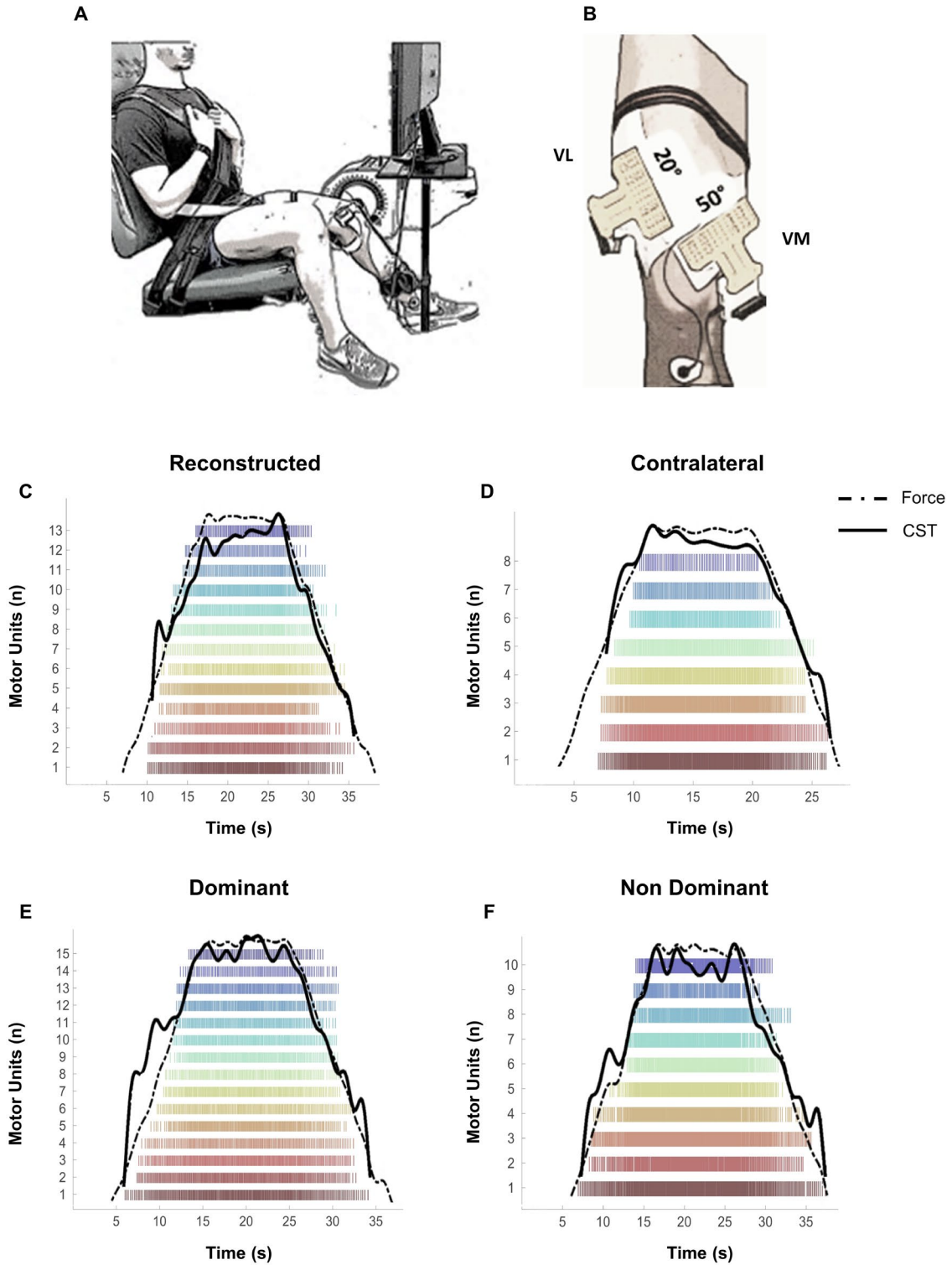

Figure 1. Experimental setup and examples of the decomposition output. Participants were seated in a dynamometer with their knee fixed at 45° of flexion (A). Two grids of 64 electrodes were attached over the VL and VM at 20° and 50° with respect to reference lines (B). Raster plots displaying the spike trains of MUs identified by the decomposition analysis from a Reconstructed (C), Contralateral (D), Dominant (E)

and Non Dominant (F) lower limb. Superimposed traces of the smoothed cumulative spike trains (CST) and Force are displayed for each trial.

Statistical analysis

The normality of the distribution was checked through the Shapiro-Wilk test. Equivalent non-parametric tests were adopted in case of non-normal data distribution. Similarly, the sphericity assumption was verified using the Mauchly's test and the Greenhouse-Geisser correction was applied in case of violation. Multiple independent t-tests were used to compare demographic characteristics between groups. All the statistical tests were performed with motor unit data averaged within each muscle (i.e., VL and VM) and lower limb (i.e., Reconstructed, Contralateral, Dominant and Non Dominant), for each participant. The overall number of identified MUs was compared among groups, sides, muscles and contraction levels using a four-way mixed model analysis of variance (ANOVA). Differences in MVIF, MU RT (absolute and relative), MU DERT (absolute and relative) and MU DR patterns were assessed using separate two-way (Side X Group) mixed-model ANOVAs. Discharge patterns of the LTMUs and HTMUs were compared between sides of the ACLR group using a two-way repeated measure ANOVA (Side x MU's type). These previous tests were run separately for VL and VM muscles and, except for MU RT-DERT, for each phase of the trapezoidal contraction. Pearson's correlation coefficients were used to examine the relationship between ΔDR_{R-T} and $\Delta Force_{R-T}$ for each participant. This analysis was performed embracing the pool of MUs extracted from the quadriceps muscle (VL + VM) to obtain an estimate of the participant-specific net synaptic input converging to the quadriceps of each lower limb. A linear regression analysis was then carried out to model this relation. Participant-specific regression slopes (i.e., rate of DR increase relative to that of Force) were compared between sides using a two-way (Side X Group) mixed-model ANOVA. To examine whether deficits in MU outputs were related to deficits in MVIF (ΔMVIF) of the ACLR group, we carried out further linear regression analyses. MU variables included in this analysis were the side-to-side difference in MU DR (ΔMU DR), MU RT (ΔMU RT) and MU DERT (ΔMU DERT). The variance between the reconstructed and the contralateral side was calculated for all variables as:

*((Contralateral – Reconstructed) / Reconstructed)*100*. The same regression analysis was conducted for the control group and the side-to-side difference was computed as *((Dominant – Non Dominant) / Non Dominant)*100*. The coefficient of determination (R^2) was computed as an index of prediction power. A Bonferroni correction was applied when needed to account for multiple comparisons. The effect size was obtained from the ANOVA and calculated as partial eta squared (ηp^2). All statistical analyses were undertaken in SPSS, Version 22.0 (SPSS Inc, Chicago, IL, USA). The significance level was set at $P<0.05$. Results are reported as mean ± SD.

RESULTS

Participant's characteristics and MVIF

The two groups were similar in terms of demographics and physical activity levels (**Table 1**). A significant between-group difference was found solely for the subjective knee function score ($P < 0.001$).

The analysis of MVIF revealed a significant Side x Group interaction ($F_{(1,17)} = 30.1$; $P < 0.001$; $\eta p^2 = 0.64$). On average, the reconstructed side was 28.7% weaker than the contralateral side (818.1 ± 131 N vs 637.8 ± 175.4 N; $t_{(9)}= -5.9$; $P = 0.0002$), whereas similar interlimb forces were observed for the control group (Dominant: 683.2 ± 106.3 N vs Non Dominant: 651.1 ± 138.5 N; $t_{(8)} = 1.4$; $P = 0.199$). In addition, there were no significant effects for Group ($F_{(1,17)} = 0.9$; $P = 0.339$; $\eta p2 = 0.054$), which indicates that the MVIFs recorded from the reconstructed and contralateral sides of the ACLR group were similar to those expressed by the dominant and non-dominant sides of the control group.

MU Decomposition

A total of 3133 MUs were identified (ACLR: n = 1517; control: n = 1616)**.** The distribution and number of MUs for each group, muscle, side, and contraction level, are shown according to their absolute and relative RT in **Figure 2.** The average number of identified MUs did not differ between groups ($P = 0.58$), sides ($P = 0.92$) or contraction levels ($P = 0.59$). By contrast, the number of identified MUs differed between muscles

(main effect for muscle; $P = 0.011$). Specifically, the number of MUs identified per participant, averaged across trials, sides and contraction levels was higher in the VL than in the VM (7.8 ± 3.6 vs 6.0 ± 2.7, respectively; $P = 0.008$).

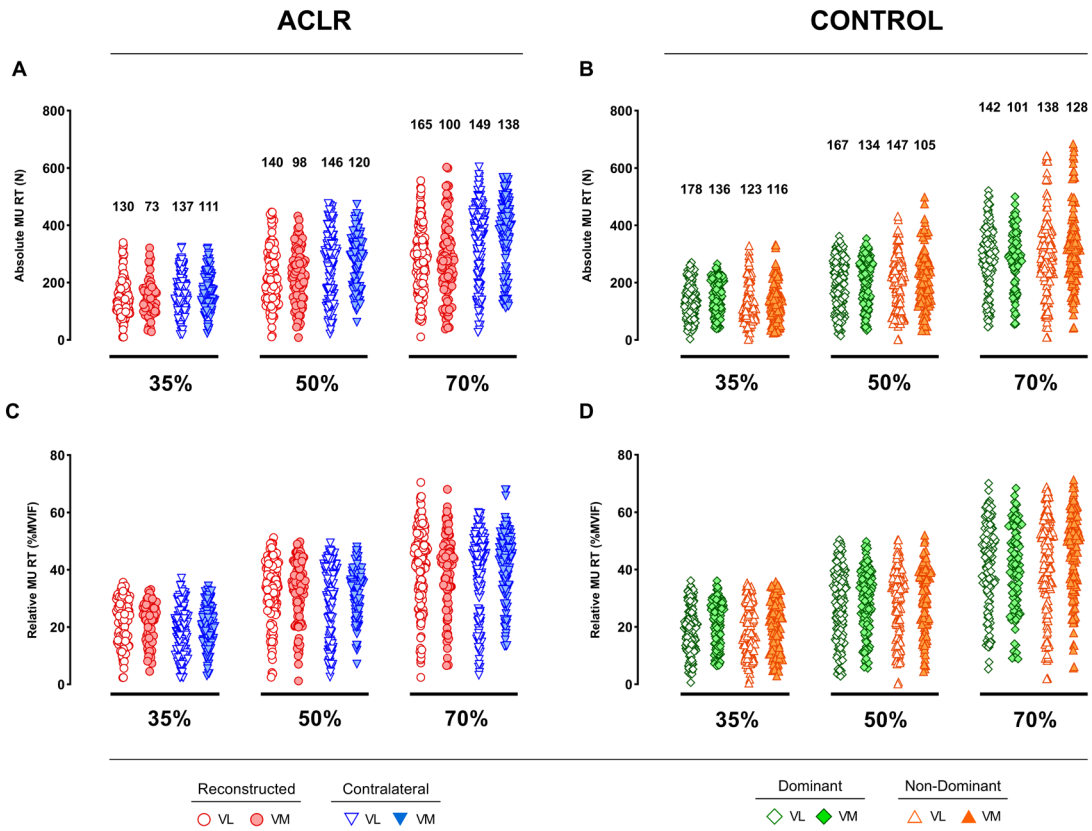

Figure 2. Number and distribution of *vasti* MUs according to their absolute and relative RT. Swarm plots representing all MUs identified for both the reconstructed and contralateral sides of the ACLR group (A-C) and for both the dominant and non-dominant sides of the control group (B-D). MUs clustered as a function of their absolute and relative RT are displayed in panels A-B and C-D, respectively.

MU Properties

MU RT and MU DERT

A significant side-to-side difference was found for the absolute MU RT and MU DERT obtained from both VL (Side x Group interaction; RT: $F_{(1,17)} = 8.0$; $P = 0.012$; $\eta p^2 = 0.32$; DERE: $F_{(1,17)} = 7.2$; $P = 0.015$; $\eta p^2 = 0.30$) and VM of the ACLR group (Side x

Group interaction; RT: $F_{(1,17)} = 10.8$; $P = 0.004$; $\eta p^2 = 0.39$; DERT: $F_{(1,17)} = 13.6$; $P = 0.002$; $\eta p^2 = 0.44$) (**Figure 3**).

On average, MUs of the VL were recruited and de-recruited at lower absolute forces on the reconstructed side compared to the contralateral side (RT: - 40.1 ± 32.9 N; -19.6%; $P = 0.004$; **Figure 3A;** DERT: - 41.6 ± 40.5 N; -19.1%; $P = 0.006$; **Figure 3E**). Similarly, the pool of MUs identified from the VM of the reconstructed side showed a 51.9 ± 49.2 N lower MU RT (-24.5%; $P = 0.009$; **Figure 3B**) and a 59.5 ± 54.3 N lower MU DERT (-25.8%; $P = 0.007$; **Figure 3F**) with respect to the contralateral side. Such a difference is probably due to inter-limb differences in the contractile properties of MUs. By contrast, MUs of the control limbs were recruited and de-recruited at similar absolute ($P > 0.05$; **Figure 3A-B-E-F**) and relative ($P > 0.05$; **Figure 3C-D-G-H**) force values. Overall, ACLR individuals showed similar MU RT and DERT to the control group in both absolute and relative values ($P > 0.05$). These results may reflect the adoption of similar MU recruitment and derecruitment strategies across limbs and groups.

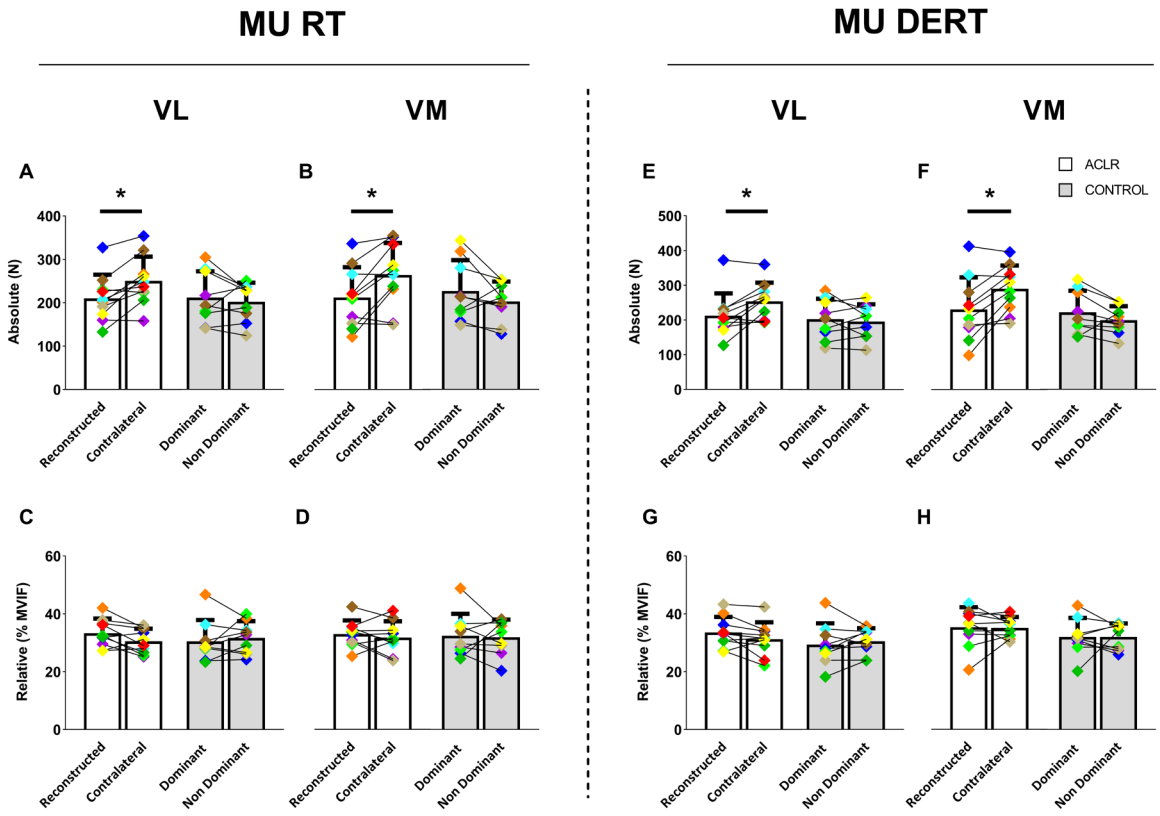

Figure 3. Differences in MU RT and MU DERT. Bar plot showing the average values for MU RT (left side) and MU DERT (right side) of the VL (A-C and E-G, respectively) and VM (B-D and F-H, respectively), across all MUs, for each participant of both the ACLR (white bars) and control (grey bars) groups. Absolute MU RT and MU DERT are reported in the upper panels. Relative MU RT and MU DERT are reported in the lower panels. Participant-specific values are displayed using diamond-shaped symbols. *$P < 0.05$.

MU DR

Participant-specific values of the average MU DR obtained from the whole trapezoidal contraction are displayed for each target force, muscle and side in **Figure 4A-B**. Significant Side x Group interactions were found for each phase of the trapezoidal contraction and for both VL (Recruitment: $\eta p^2 = 0.22$; $P = 0.042$; Plateau: $\eta p^2 = 0.62$; $P < 0.001$) and VM muscles (Recruitment: $\eta p^2 = 0.36$; $P = 0.007$; Plateau: $\eta p^2 = 0.55$; $P < 0.001$; De-recruitment: $\eta p^2 = 0.32$; $P = 0.012$), except for the derecruitment phase of VL ($P = 0.10$). Specifically, the mean DR expressed by MUs of the reconstructed side was significantly lower than the contralateral side at recruitment (VL: - 1.4 ± 1.5 pps; -20.1 %; $P = 0.024$; VM: - 1.9 ± 1.0 pps; -29.1 %; $P = 0.001$; **Figure 4C-F)** plateau (VL: - 2.0 ± 0.8 pps; -19.1 %; $P < 0.001$; VM: -2.7 ± 1.2 pps; -25.4 %; $P < 0.001$; **Figure 4D-G**) and de-recruitment (VM: - 0.8 ± 0.8 pps; -14.6 %; $P = 0.02$; **Figure 4E-H**). No significant side-to-side differences were found for the control group ($P > 0.05$). Overall, mean MU DR values of the ACLR group were similar to the values expressed by the control group for both VL ($P = 0.79$) and VM ($P = 0.33$) muscles.

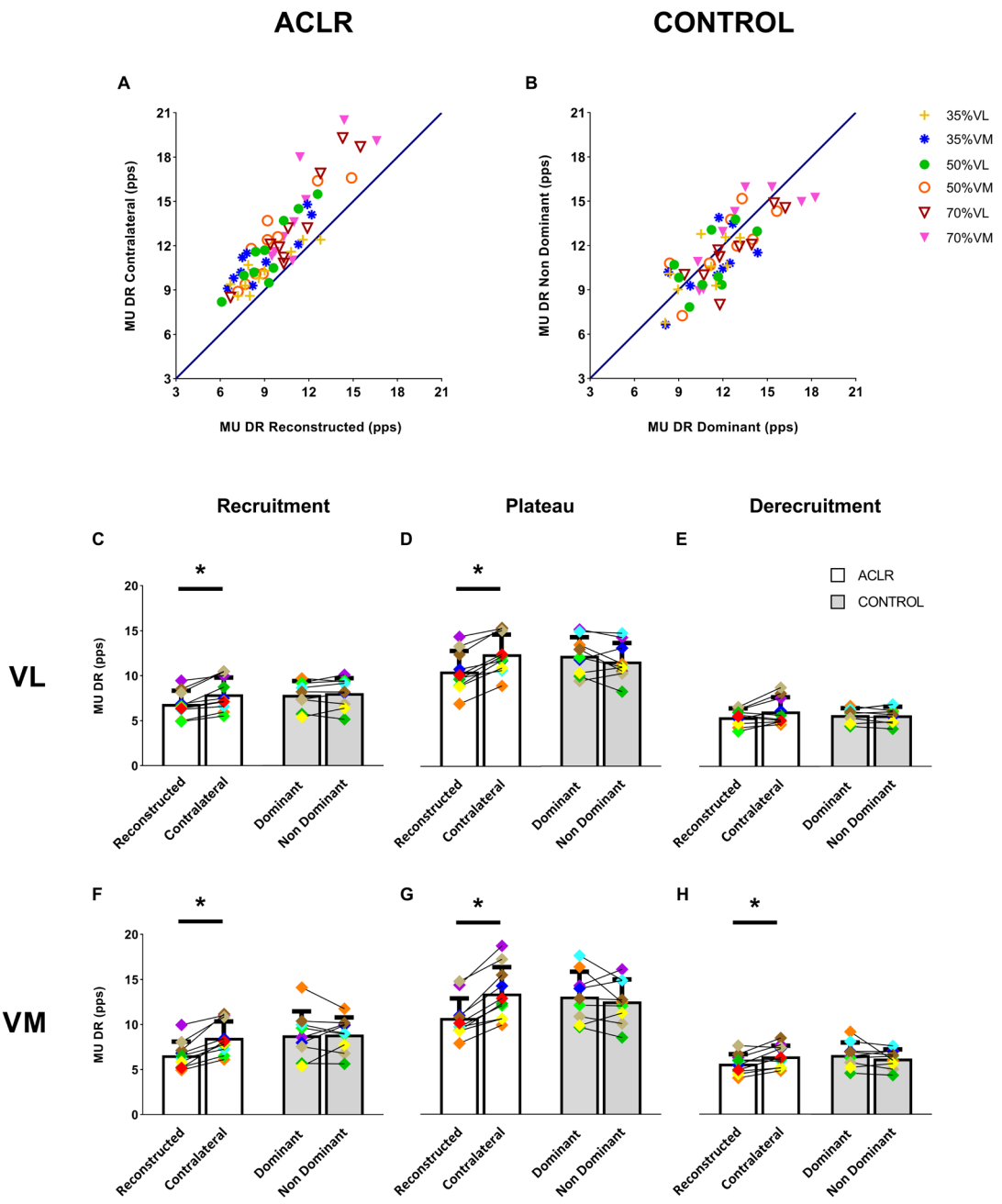

Figure 4. Differences in MU DR. Scatter plots representing the mean MU DR (averaged across the whole trapezoidal contraction) of the VL and VM, for each target force and participant of both the ACLR (A; reconstructed *vs* contralateral side) and control (B; dominant *vs* non-dominant) groups. Bar plots showing the average MU DR at recruitment (C and F for VL and VM, respectively), plateau (D and G for VL and VM ,respectively) and derecruitment (E and H for VL and VM, respectively), for both the ACLR (white bars) and control (grey bars) groups. Participant-specific values are displayed using diamond-shaped symbols.*$P < 0.05$

Figure 5 shows the DR expressed by MUs of the ACLR group, clustered according to their RT and graphed separately for each phase, contraction level and muscle. The analysis of MU DR as a function of MU RT was adopted to assess the relative contribution of LTMUs (< 30% MVIF) and HTMUs (≥ 30% MVIF) to side-to-side deficits in MU DR. Significant Side x MU's type interactions were found for the VL at recruitment ($P = 0.003$; $\eta p^2 = 0.65$), whilst significant side effects were found for each phase of the trapezoidal contraction in the VM ($P < 0.05$) and for the plateau phase in the VL ($P < 0.001$; $\eta p^2 = 0.87$). The reduced excitatory input received by the VL of the reconstructed side with respect to the contralateral side at recruitment was due to a selective impairment of the HTMUs (- 28.6%; $P < 0.001$; **Figure 5-G**). At plateau, both LTMUs and HTMUs significantly contributed to side-to-side differences in MU DR of the VL (LTMUs: - 15.2%; $P = 0.014$; HTMUs: - 20.6%; $P < 0.001$). For the VM (**Figure 5-H**), the DR of both LTMUs and HTMUs was significantly lower in the reconstructed side compared to the contralateral side at recruitment (LTMUs: - 19.4%, $P = 0.006$; HTMUs: - 37%, $P = 0.002$) and plateau (LTMUs: - 21.4%, $P = 0.001$; HTMUs: - 30.9%, $P = 0.001$). At derecruitment, only the LTMUs were significantly affected (LTMUs: - 14.1%, $P = 0.014$).

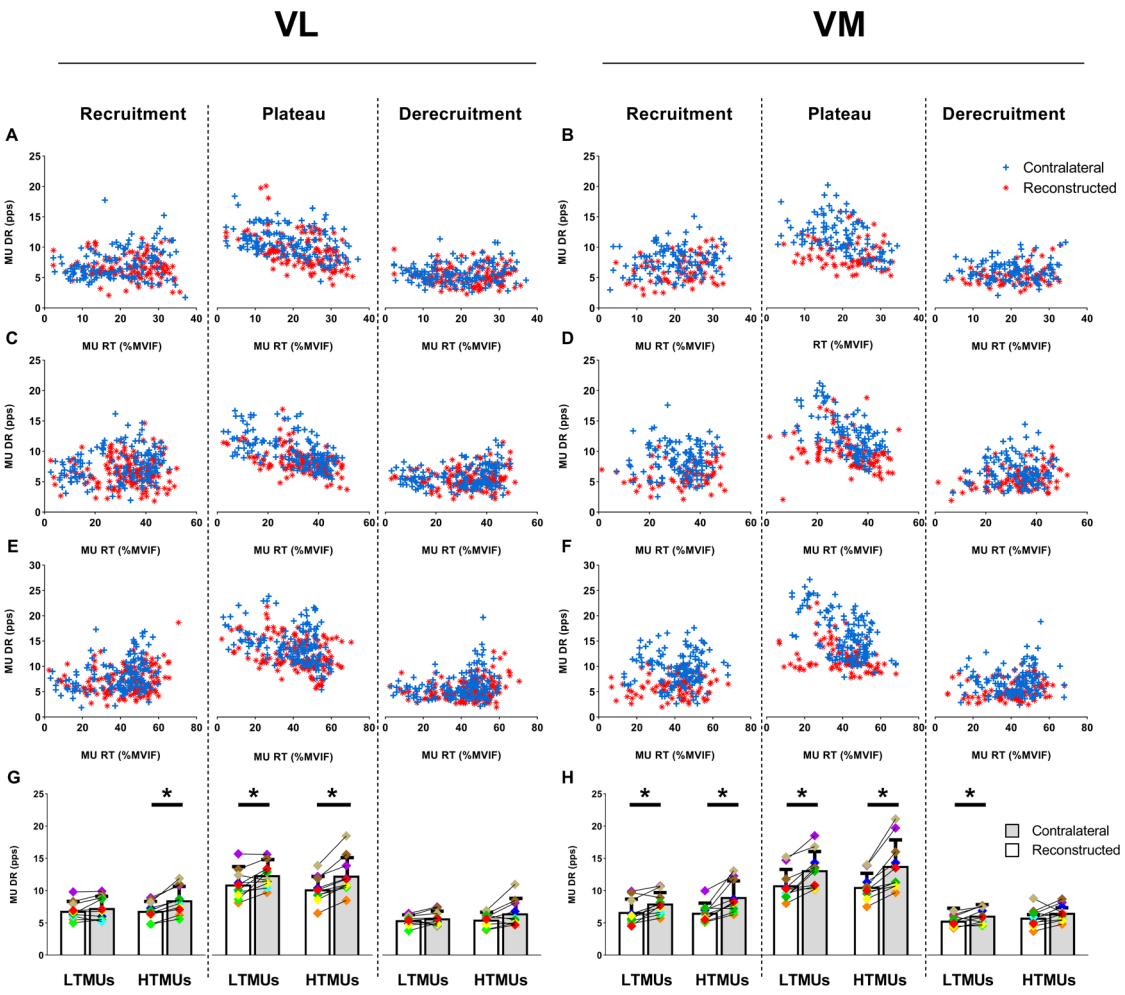

Figure 5. Differences in MU DR for LTMUs and HTMUs of the ACLR group. Scatter plots showing the DR of all identified MUs from both the reconstructed and contralateral sides. MUs are clustered according to their RT, displayed separately for each phase of the trapezoidal contraction (i.e., recruitment, plateau, derecruitment) and for each force target (35% of MVIF in panels A-B; 50% of MVIF in panels C-D; 70% of MVIF in panels E-F). Differences between the reconstructed (white bars) and the contralateral side (grey bars) in MU DR of both LTMUs (MU RT < 30% MVIF) and HTMUs (MU RT ≥ 30% MVIF) are reported for both the VL and the VM in panels G and H, respectively. Participant-specific values in panels G-H are displayed using diamond-shaped symbols. *$P < 0.05$*

Input-output gain of the vasti motoneuron pool

An estimation of the synaptic input converging to *vasti* motoneurons was obtained by examining the relation between the change in MU DR ($\Delta DR_{R\text{-}T}$: from recruitment to

target force) with respect to the change in volitional force ($\Delta Force_{R\text{-}T}$: from recruitment to the target) in both the VL and VM muscles. $\Delta DR_{R\text{-}T}$ and $\Delta Force_{R\text{-}T}$ were linearly correlated in all participants and muscles, in both absolute (N) and relative (%MVIF) values. Participant-specific slopes of the regression lines, representing the rate of change in MU DR as a function of the rate of change in Force, were, on average, significantly lower for the reconstructed side than the contralateral side, only when considering relative force values (Relative Force: $P = 0.009$; **Figure 6F;** Absolute force: $P > 0.05$; **Figure 6C**). No inter-limb differences were found for the control group ($P > 0.05$ **Figure 6C-F**). Furthermore, no differences were found between the ACLR and control groups, in both absolute and relative values ($P > 0.05$; **Figure 6C-F**). Collectively, these results suggest a reduced net excitatory input to the pool of *vasti* motoneurons on the reconstructed side and a consequent reduction in the effective neural drive to the muscles.

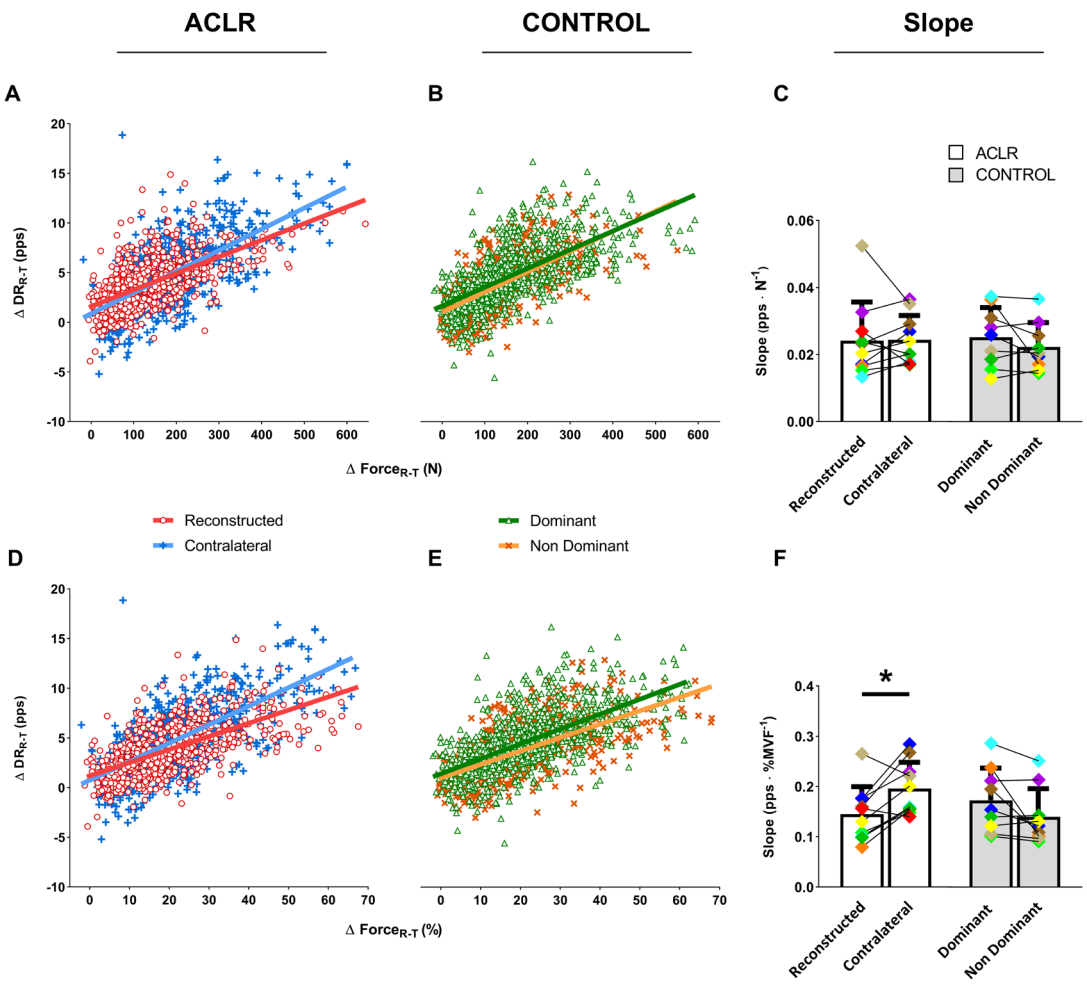

Figure 6. Differences in the input-output gain of the *vasti* motoneuron pool. Scatter plots showing the change in knee extensor's force ($\Delta Force_{R-T}$ from recruitment to target) as a function of the change in MU DR (ΔMU DR_{R-T} from recruitment to target) of all *vasti* MUs identified in both the ACLR (A-D), and control group (B-E). $\Delta Force_{R-T}$ is expressed in both absolute (A-B) and relative values (D-E). Regression lines are reported for each lower limb for absolute (Reconstructed: R^2 =0.35; Contralateral: R^2 =0.44; Dominant: R^2 =0.41 Non Dominant: R^2 =0.42) and relative forces (Reconstructed: R^2 =0.41; Contralateral: R^2 =0.47; Dominant: R^2 =0.41 Non Dominant: R^2 =0.38). Bar plots in panels C and F show the absolute and relative slopes (rate of change of MU DR as a function of the rate of change of Force) of the regression lines obtained for each participant, respectively. Participant-specific values in panels C-F are displayed using diamond-shaped symbols.*$P= 0.009$

Determinants of deficits in MVIF

Linear regression analyses were adopted to identify potential MU variables related to deficits in MVIF of the ACLR group. We found a strong and linear correlation between the relative side-to-side difference in MVIF (ΔMVIF) and the relative side-to-side difference in mean MU DR (ΔMUDR) of the VL (R^2 = 0.44; P = 0.04; **Figure 7A**). In addition, as shown in **Figure 7B** and **7C**, ΔMVIF was significantly related with the ΔMUDR of the VL obtained during the recruitment (R^2 = 0.49; P = 0.02) and plateau (R^2 = 0.49; P = 0.02) phases of the trapezoidal contraction. In contrast to the VL, no significant associations (P > 0.05) were found between ΔMVIF and ΔMUDR for the VM muscle (**Figure 7E-F-G-H**). These results suggest that deficits in MU DR of the VL strongly contribute to weakness in knee extension strength following ACLR. Similarly, for the control group, the ΔMVIF was significantly correlated with ΔMUDR of the VL at recruitment (R^2 = 0.55; P = 0.02), plateau (R^2 = 0.60; P = 0.01) and when considering the whole trapezoidal contraction (R^2 = 0.67; P = 0.007), whilst no associations were found for the VM, except for ΔMUDR at recruitment (R^2 = 0.56; P = 0.02).

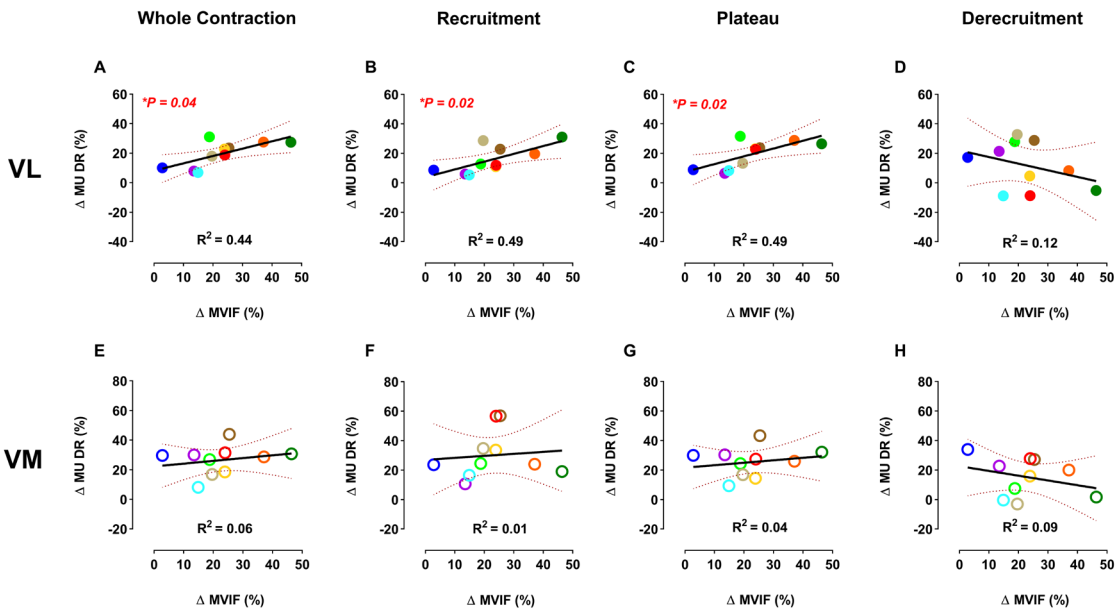

Figure 7. Relations between ΔMU DR and ΔMVIF for the ACLR group. Scatter plots showing the association between the relative side-to-side difference in MU DR (ΔMU DR) and the relative side-to-side difference in MVIF (ΔMVIF) for the ACLR group. The linear regression analysis was carried out for the average MU DR of the whole trapezoidal contraction (A-E for VL and VM, respectively), recruitment (B-F for VL and VM, respectively), plateau (C-G for VL and VM, respectively) and derecruitment (D-H for VL and VM, respectively) phases. Participant-specific values for the VL and VM are displayed using filled and empty circles, respectively.

To assess whether deficits in MU DR of the VL were uniform across ACLR participants, we further examined the relation between MU DR of the reconstructed side *vs* the contralateral side. Interestingly, the average MU DR of the reconstructed side explained the 89.7% of the variance in MU DR of the contralateral side (P <0.001; **Figure 8A**). Strong and significant associations were additionally observed for each phase of the trapezoidal contraction (P < 0.001; **Figure 8B-C-D**), suggesting that deficits in MU DR of the VL were uniform across our sample of ACLR individuals.

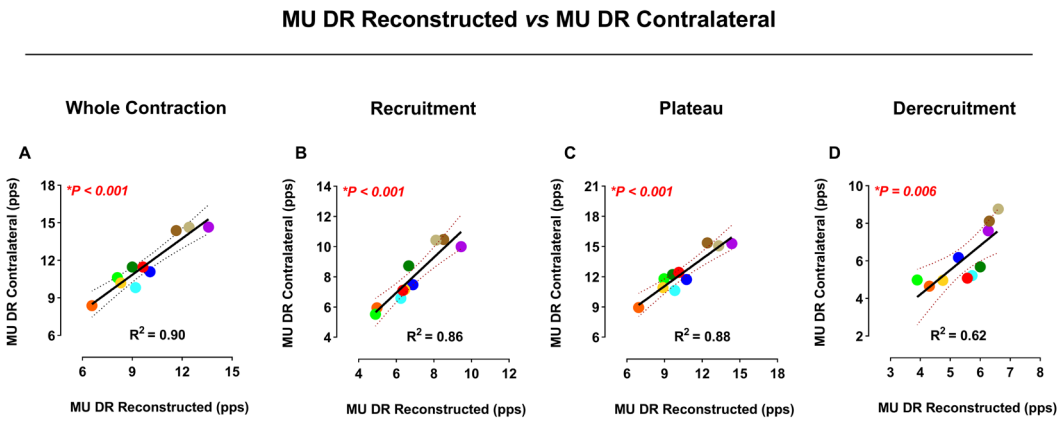

414

415 **Figure 8**. **Uniform deficit in MU DR of the VL across ACLR participants**. Scatter plots showing the
416 association between the average MU DR of the reconstructed side and the average MU DR of the
417 contralateral side for the VL, across all MUs and target forces. The linear regression analysis was carried
418 out for the average MU DR of the whole trapezoidal contraction (A), recruitment (B), plateau (C) and
419 derecruitment (C) phases. Participant-specific values are displayed using filled circles.

420

421 **Figure 9** depicts the relations between ΔMVIF and both ΔMU RT and ΔMU DERT for
422 the ACLR group. ΔMVIF was significantly correlated with the absolute ΔMU RT and
423 ΔMU DERT in both the VL (ΔMU RT: $R^2 = 0.50$; $P = 0.02$; ΔMU DERT: $R^2 = 0.60$; P
424 $= 0.008$; **Figure 9A** and **9C**, respectively) and the VM (ΔMU RT: $R^2 = 0.69$; $P = 0.003$;
425 ΔMU DERT: $R^2 = 0.68$; $P = 0.003$; **Figure 9E** and **9G**, respectively). Conversely, no
426 significant correlations were found for relative ΔMU RT ($P > 0.05$; Figure 9B-F) and
427 ΔMU DERT ($P > 0.05$; Figure 9D-H). These findings suggest that differences in the
428 peripheral properties of *vasti* MUs (e.g., reduced twitch forces) may partly explain the
429 observed weakness of the knee extensor muscles. The regression analyses for the
430 control group revealed no significant associations between ΔMVIF and both absolute
431 and relative ΔMU RT ($P > 0.05$) and ΔMU DERT ($P > 0.05$).

432

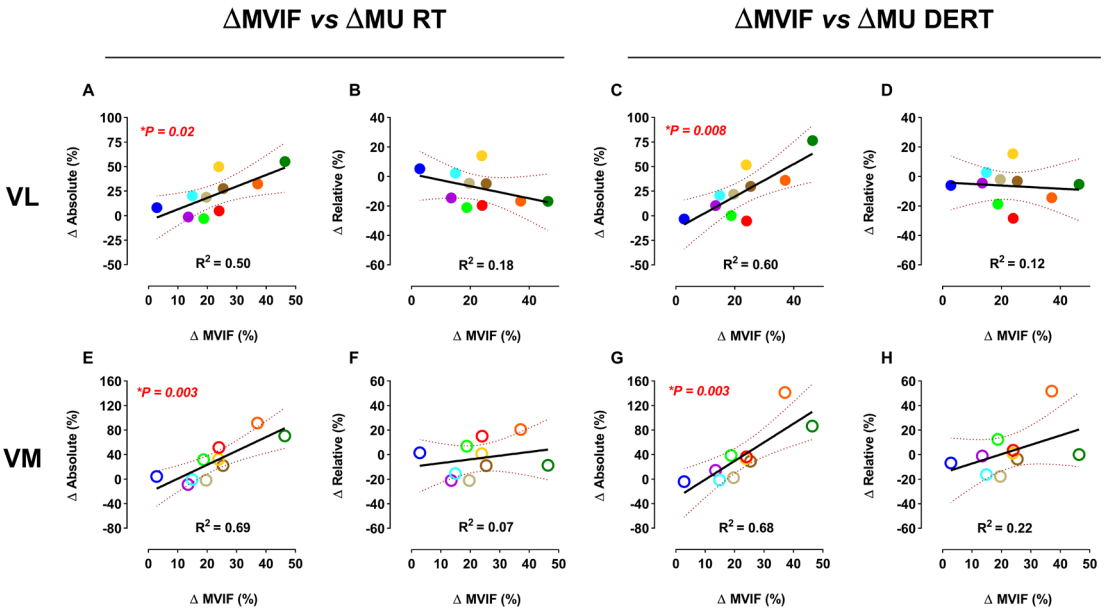

Figure 9. Relations between ΔMVIF and both ΔMU RT and ΔMU DERT for the ACLR group. Scatter plots showing the linear regressions between both the relative side-to-side difference in MU RT and MU DERT (ΔMU RT and Δ MU DERT) and the relative side-to-side difference in MVIF (ΔMVIF) for the ACLR group. The regression analysis was carried out for both the absolute ΔMU RT (A-E for VL and VM, respectively) and ΔMU DERT (C-G for VL and VM, respectively), as well as for both the relative ΔMU RT (B-F for VL and VM, respectively) and ΔMU DERT (D-H for VL and VM, respectively). Participant-specific values for the VL and VM are displayed using filled and empty circles, respectively.

DISCUSSION

The present study demonstrated, for the first time, that deficits in knee extension strength following ACLR are explained by deficits in spinal motoneuronal output (i.e., neural drive to the *vasti* muscles). We found lower knee extensor MVIFs on the reconstructed side with respect to the contralateral side, which were accompanied by deficits in MU DR and by reduced absolute MU RT and DERT during submaximal force contractions. In addition, we found an altered input-output gain for the entire pool of *vasti* motoneurons, which potentially reflects reduced excitatory (i.e., descending command) and/or increased inhibitory (i.e., afferent feedback) inputs to motoneurons. An inhibitory-facilitated reduction in motoneuronal intrinsic excitability and changes at

muscle unit level may have contributed to deficits in MU DR and MU RT-DERT, respectively. In contrast to our hypothesis, no significant differences in MVIF and MU properties were found between the ACLR and the control group, potentially due to the bilateral neuromuscular gain (i.e., increased MVIF and MU DR) (Del Vecchio *et al.*, 2019) that was achieved by the ACLR group following the specific strength training program of the knee extensors that they underwent during the rehabilitation process.

The force produced by a given muscle depends on the contractile properties of muscle units and on the ensemble output of motoneurons which, in turn, is determined by recruitment and rate coding. Our sample of ACLR individuals showed no significant alterations in both relative MU RT and DERT (**Figure 3**), which may suggest that the neural strategies modulating the number of MUs to be activated and deactivated during submaximal force contractions did not change following ACLR. Conversely, we found significantly lower absolute RT (VL: - 19.6%; VM: - 24.5%) and DERT (VL: - 19.1%; VM: - 25.8%) on the reconstructed side with respect to the contralateral side which were strongly related with deficits in MVIF (**Figure 9**). Reduced absolute recruitment and derecruitment thresholds are consistent with peripheral motor unit adaptations (Van Cutsem *et al.*, 1997). Specifically, it is plausible that the contractile properties of *vasti* MUs (e.g., twitch forces) were affected and that changes occurring at the muscle unit level may have contributed to the reduced force-generating capacity of the reconstructed side. The reduced DR at recruitment and derecruitment further support this hypothesis. In addition, in a previous study, we observed reduced muscle fibre conduction velocities following ACL surgery which may reflect alterations in muscle fibre's diameter and sarcolemmal excitability (Nuccio *et al.*, 2020). Moreover, there is evidence for mid-to-long term changes in quadriceps morphology (Flück *et al.*, 2018; Lepley *et al.*, 2019; Birchmeier *et al.*, 2020) and architecture (Noehren *et al.*, 2016) following ACL surgery. For instance, Noehren et al. (2016), reported a significant deficit in quadriceps strength at an average of six months post-surgery that was accompanied by a decreased physiological cross-sectional area, an increased abundance of hybrid type IIa/X muscle fibres and a decreased frequency of type IIa muscle fibres. Therefore, alterations at the muscle unit level are plausible and seem to coexist with the impairments at a motoneuronal level.

The main neural mechanism contributing to the lower MVIF of the reconstructed side with respect to the contralateral was the lower MU DR expressed by MUs of the VL (**Figure 7**). We observed deficits in MU DR at recruitment (VL: - 20.1%; VM: - 29.1%), plateau (VL: - 19.1%; VM: - 25.4%) and derecruitment phases (VM: - 14.6%) of the submaximal trapezoidal contractions (**Figure 4**). Interestingly, although the MU DR at plateau of both HTMUs and LTMUs was reduced in both muscles, deficits in MU DR at recruitment and derecruitment were due to alterations of HTMUs, for the VL, and of both HTMUs and LTMUs, for the VM (**Figure 5**). Despite this muscle-specific adaptation in MU DR, the weakness of the knee extensors was only predicted by deficits in MU DR of the VL (**Figure 7**). Therefore, at recruitment, only the reduced MU DR of the HTMU and not of LTMUs may be of clinical relevance.

The frequency at which motoneurons discharge their action potentials is proportional to the net synaptic input received by motoneurons and is modulated by the intrinsic properties of motoneurons (Heckman & Enoka, 2012). Motoneuronal inherent factors such as monoamine-facilitated (i.e. neuromodulation) persistent inward currents (PICs) are known to sharply increase (up to five-fold) the excitability of motoneurons and, as a consequence, the MU DR when motoneurons are first activated (Heckman *et al.*, 2008; Heckman & Enoka, 2012). Interestingly, increased inhibitory afferent inputs (i.e. recurrent and reciprocal inhibition) can markedly depress PICs resulting in reduced MU DRs at recruitment (Hyngstrom *et al.*, 2007; Revill & Fuglevand, 2017). Accordingly, although there is no evidence for changes in reciprocal and Renshaw cell-mediated recurrent inhibition following ACLR, the well-documented inability to fully activate the knee extensor muscles after a joint trauma (Rice & McNair, 2010) may potentially underlie intrinsic motoneuronal alterations. Specifically, inhibitory mechanisms such as Ib nonreciprocal inhibition, gamma-loop dysfunction and flexion-reflex could be facilitated by peripheral alterations (i.e., disruption of articular receptors after a joint trauma), in order to reduce the stress to the damaged joint (Konishi *et al.*, 2002; Rice & McNair, 2010; Krogsgaard *et al.*, 2011; Needle *et al.*, 2017). Based on this assumption, an inhibitory-induced PICs deactivation is plausible and could partially explain the between-side difference in MU DR at recruitment observed in the ACLR group. However, these parameters were not directly investigated in the current study

and further research is needed to clarify their contribution to quadriceps weakness after injury.

To support the hypothesis of a substantial neural impairment affecting the activity of *vasti* motoneurons following ACLR, we estimated the input-output gain of the entire pool of *vasti* MUs. Participant-specific slopes resulting from the relationship between ΔMU $DR_{R\text{-}T}$ (MU DR at target force minus MU DR at recruitment) with respect to the relative $\Delta Force_{R\text{-}T}$ (target force minus RT) were significantly lower on the reconstructed side than on the contralateral side, thus reflecting an overall reduction in the net excitatory input to motoneurons of the reconstructed side (**Figure 6**). The synaptic input received by motoneurons represents the sum of both excitatory and inhibitory inputs from afferent and descending neural pathways that are ultimately processed and transduced into the effective neural drive to the muscle (Heckman & Enoka, 2012). Accordingly, whether the neural deficit of the reconstructed side is the result of a more reduced corticospinal excitability, rather than alterations in spinal or afferent circuits cannot be inferred from this analysis. Previous investigations reported ACLR-related neural alterations at cortical (Lepley *et al.*, 2015; Grooms *et al.*, 2017; Lisee *et al.*, 2019), spinal (Lepley *et al.*, 2015) and peripheral levels (Krogsgaard *et al.*, 2011). A longitudinal study conducted by Lepley and colleagues (2015) demonstrated a different time-course of the neural changes following ACLR with a reduced spinal reflex excitability occurring early following surgery and deficits in corticospinal excitability occurring during the latest stages of rehabilitation (about six months post-surgery). In another study, Lepley et al. (2019) corroborated these findings, reporting that persistent deficits in quadriceps strength after ACL surgery were accompanied by unaltered Hoffman reflex values, increased active motor threshold (AMT), decreased motor evoked potentials (MEP) and greater activation in the frontal areas of the brain measured through fMRI. Collectively these results highlighted the presence of significant neuroplasticity which was accompanied by an impaired excitability of neurons within the primary motor cortex (i.e., increased AMT) and a consequent reductions in the effective neural drive to the muscle (i.e., decreased MEP) (Lepley *et al.*, 2019). In accordance with these studies, the reduced input-output motoneuron gain found in the current investigation could reflect a reduced excitatory input from supraspinal centres. However, an increased synaptic inhibition due to both AMI-related

changes in the afferent feedback and dysfunctions of the gamma-loop may have contributed to this finding (Konishi *et al.*, 2002; Rice & McNair, 2010; Needle *et al.*, 2017).

The comparison between the participant-specific slopes of the regression lines obtained from the estimation of the input-output gain with absolute forces revealed no differences between the lower limbs of the ACLR group, indicating that for the same level of absolute rate of change in force (i.e., output) the rate of change in MU DR (i.e., input) was similar (**Figure 6**). Although this finding would suggest no side-to side differences in muscle efficiency (i.e., similar neural input needed to exert similar absolute forces) and a potential intrinsic compensation of the quadriceps muscle to the neural impairment, the significant differences in MVIF and absolute MU RT between the reconstructed and contralateral sides question this interpretation.

A compelling finding of this study was the strong and linear relation found between the MU DR of the VL in the reconstructed side with that of the contralateral side (**Figure 8**). If coupled with the strong correlation found between ΔMVIF and ΔMU DR of the same muscle, this observation suggests that several months following ACLR a) the neural deficit underlying the weakness of the knee extensors is uniform across ACLR individuals and b) the deficit in the neural drive to the VL is predictive and proportional to that of MVIF. Although the small sample involved in this study does not allow strong generalizations, this finding may open novel perspectives in the field of rehabilitation after ACLR. For instance, the identification of potential neurophysiological markers of the ACLR-related knee extensor's weakness may help to improve rehabilitation protocols aimed at restoring quadriceps strength and function.

Furthermore, the findings from our study indicate that deficits in knee extension strength are predicted by neural deficits of the VL and not VM (**Figure 7**). Such an inter-muscle difference may have an impact in clinical contexts. The VM is usually considered as the main rehabilitation target to fully recover knee extension strength after ACLR. This is because a weak VM leads to alterations in patellofemoral biomechanics which, as a consequence, may increase patellofemoral pain (a factor inducing arthrogenic quadriceps inhibition following ACLR) (Buckthorpe *et al.*, 2019). However,

in accordance with our findings, treating the neuromuscular deficits of the VL is essential to restore a symmetric knee extension strength. Therefore, clinical professionals should be aware of the importance of the VL and should consider its full recovery as a main target when prescribing post-surgery rehabilitation protocols.

Some limitations should be considered. First, the cross-sectional design of the present investigation does not allow to consider the clinical and neurological progresses of the quadriceps throughout the rehabilitation process following ACLR. Therefore, longitudinal studies investigating changes in the behaviour of motor units from pre-surgery to the latest stages of rehabilitation are warranted (Enoka, 2019). Second, our results suggest a bilateral gain in knee extension strength and MU outputs of the ACLR group (i.e., no differences with control lower limbs). Therefore, the neural impairment of the reconstructed side may be overestimated, as we could not determine the extent of the potential gain in both MVIF and MU DR of the contralateral side. However, regardless of this potential confounding effect, we found a persistent between-side deficit in MVIF which represents a key issue to solve in order to reduce the risk of further knee injuries (Grindem *et al.*, 2016; Kyritsis *et al.*, 2016). Third, the different subject-specific number of MUs that have been identified within trials (i.e., HTMUs/LTMUs) and across trials (i.e., MUs at 30-50-70% of MVIF) may have affected the distribution of MUs, resulting in a high between-participant variability in MU DRs. Lastly, the potential sources (i.e., supraspinal, spinal or peripheral) and their differential contribution to MU adaptations remain to be elucidated.

In conclusion, we demonstrated that the persistent deficit in knee extension strength following ACLR is related to a reduced neural drive to the *vasti* muscles. The uniform deficit in MU DR of the VL and the reduced absolute MU RT and DERT were identified as main determinants. Additionally, we documented alterations in the input-output motoneuronal relation which suggest synaptic alterations due to either a reduced net excitatory input (i.e., altered descending command) or increased inhibitory afferent inputs to spinal motoneurons.

REFERENCES

Barbero M, Merletti R & Rainoldi A (2012). *Atlas of Muscle Innervation Zones*. Springer Milan, Milano.

Birchmeier T, Lisee C, Kane K, Brazier B, Triplett A & Kuenze C (2019). Quadriceps Muscle Size Following ACL Injury and Reconstruction: A Systematic Review. *J Orthop Res* **38**, 598-608.

Buckthorpe M, La Rosa G, Villa FD (2019). Restoring Knee Extensor Strength After Anterior Cruciate Ligament Reconstruction: A Clinical Commentary. *Int J Sports Phys Ther* **14**, 159-172.

Bryant AL, Kelly J & Hohmann E (2008). Neuromuscular adaptations and correlates of knee functionality following ACL reconstruction. *J Orthop Res* 26, 126-135.

Casolo A, Farina D, Falla D, Bazzucchi I, Felici F & Del Vecchio A (2020). Strength Training Increases Conduction Velocity of High-Threshold Motor Units. *Med Sci Sport Exerc* **52,** 955–967.

Castronovo M, Mrachacz-Kersting N, Landi F, Jørgensen HR, Severinsen K & Farina D (2017). Motor Unit Coherence at Low Frequencies Increases Together with Cortical Excitability Following a Brain-Computer Interface Intervention in Acute Stroke Patients. In *In Converging Clinical and Engineering Research on Neurorehabilitation II (pp. 1001-1005). Springer, Cham*.

Del Vecchio A, Casolo A, Negro F, Scorcelletti M, Bazzucchi I, Enoka R, Felici F & Farina D (2019). The increase in muscle force after 4 weeks of strength training is mediated by adaptations in motor unit recruitment and rate coding. *J Physiol* **597**, 1873–1887.

Del Vecchio A, Holobar A, Falla D, Felici F, Enoka RM & Farina D (2020). Tutorial: Analysis of motor unit discharge characteristics from high-density surface EMG signals. *J Electromyogr Kinesiol* **53**, 102426.

Del Vecchio A, Ubeda A, Sartori M, Azorin JM, Felici F, Farina D (2018). Central nervous system modulates the neuromechanical delay in a broad range for the control of muscle force. *J Appl Physiol*. **125**, 1404-10.

Enoka RM (2019). Physiological Validation of the Decomposition of Surface EMG Signals. *J Electromyogr Kinesiol* **46**, 70-83.

Flück M, Viecelli C, Bapst AM, Kasper S, Valdivieso P, Franchi M V., Ruoss S, Lüthi J-M, Bühler M, Claassen H, Hoppeler H & Gerber C (2018). Knee Extensors Muscle Plasticity Over a 5-Years Rehabilitation Process After Open Knee Surgery. *Front Physiol* **9**, 1343.

Grindem H, Snyder-Mackler L, Moksnes H, Engebretsen L & Risberg MA (2016). Simple decision rules can reduce reinjury risk by 84% after ACL reconstruction: The Delaware-Oslo ACL cohort study. *Br J Sports Med* **50,** 804–808.

Grooms DR, Page SJ, Nichols-Larsen DS, Chaudhari AMW, White SE & Onate JA (2017). Neuroplasticity Associated With Anterior Cruciate Ligament Reconstruction. *J Orthop Sport Phys Ther* **47,** 180–189.

Hart JM, Pietrosimone B, Hertel J & Ingersoll CD (2010). Quadriceps activation following knee injuries: A systematic review. *J Athl Train* **45,** 87–97.

Heckman CJ & Enoka RM (2012). Motor Unit. *Compr Physiol* **2,** 2629–2682.

Heckman CJ, Johnson M, Mottram C & Schuster J (2008). Persistent inward currents in spinal motoneurons and their influence on human motoneuron firing patterns. *Neuroscientist* **14**, 264-275.

Herrington L, Ghulam H & Comfort P (2021). Quadriceps Strength and Functional Performance After Anterior Cruciate Ligament Reconstruction in Professional Soccer players at Time of Return to Sport. *J Strength Cond Res* **35**, 769-775.

Holobar A, Minetto MA & Farina D (2014). Accurate identification of motor unit discharge patterns from high-density surface EMG and validation with a novel signal-based performance metric. *J Neural Eng* **11,** 016008.

Holobar A & Zazula D (2007). Multichannel blind source separation using convolution Kernel compensation. *IEEE Trans Signal Process* **55,** 4487–4496.

Hyngstrom AS, Johnson MD, Miller JF & Heckman CJ (2007). Intrinsic electrical properties of spinal motoneurons vary with joint angle. *Nat Neurosci* **10,** 363–369.

Ingersoll CD, Grindstaff TL, Pietrosimone BG & Hart JM (2008). Neuromuscular Consequences of Anterior Cruciate Ligament Injury. *Clin Sports Med* **27**, 383-404.

664 Konishi Y, Fukubayashi T & Takeshita D (2002). Mechanism of quadriceps femoris
665 muscle weakness in patients with anterior cruciate ligament reconstruction. *Scand*
666 *J Med Sci Sport* **12**, 371-375.

667 Krogsgaard MR, Fischer-Rasmussen T & Dyhre-Poulsen P (2011). Absence of sensory
668 function in the reconstructed anterior cruciate ligament. *J Electromyogr Kinesiol*
669 **21,** 82–86.

670 Kuenze CM, Hertel J, Weltman A, Diduch D, Saliba SA & Hart JM (2015). Persistent
671 neuromuscular and corticomotor quadriceps asymmetry after anterior cruciate
672 ligament reconstruction. *J Athl Train* **50,** 303–312.

673 Kyritsis P, Bahr R, Landreau P, Miladi R & Witvrouw E (2016). Likelihood of ACL
674 graft rupture: not meeting six clinical discharge criteria before return to sport is
675 associated with a four times greater risk of rupture. *Br J Sports Med* **50**, 946-951.

676 Labanca L, Rocchi JE, Laudani L, Guitaldi R, Virgulti A, Mariani PP & Macaluso A
677 (2018). Neuromuscular Electrical Stimulation Superimposed on Movement Early
678 after ACL Surgery. *Med Sci Sports Exerc* **50**, 407-416.

679 Lepley AS, Gribble PA, Thomas AC, Tevald MA, Sohn DH & Pietrosimone BG
680 (2015). Quadriceps neural alterations in anterior cruciate ligament reconstructed
681 patients: A 6-month longitudinal investigation. *Scand J Med Sci Sport* **25,** 828–
682 839.

683 Lepley AS, Grooms DR, Burland JP, Davi SM, Kinsella-Shaw JM & Lepley LK
684 (2019). Quadriceps muscle function following anterior cruciate ligament
685 reconstruction: systemic differences in neural and morphological characteristics.
686 *Exp Brain Res* **237,** 1267–1278.

687 Lisee C, Lepley AS, Birchmeier T, O'Hagan K & Kuenze C (2019). Quadriceps
688 Strength and Volitional Activation After Anterior Cruciate Ligament
689 Reconstruction: A Systematic Review and Meta-analysis. *Sports Health* **11,** 163–
690 179.

691 Needle AR, Lepley AS & Grooms DR (2017). Central Nervous System Adaptation
692 After Ligamentous Injury: a Summary of Theories, Evidence, and Clinical
693 Interpretation. *Sport Med* 47, 1271-1288.

694 Noehren B, Andersen A, Hardy P, Johnson DL, Ireland ML, Thompson KL & Damon B
695 (2016). Cellular and morphological alterations in the vastus lateralis muscle as the
696 result of ACL injury and reconstruction. *J Bone Jt Surg - Am Vol* **98,** 1541–1547.

697 Nuccio S, Del Vecchio A, Casolo A, Labanca L, Rocchi JE, Felici F, Macaluso A,
698 Mariani PP, Falla D, Farina D & Sbriccoli P (2020). Muscle fiber conduction
699 velocity in the vastus lateralis and medialis muscles of soccer players after ACL
700 reconstruction. *Scand J Med Sci Sports* **30**, 1976-1984.

701 Palmieri-Smith R, & Thomas, AC (2009). A neuromuscular mechanism of
702 posttraumatic osteoarthritis associated with ACL injury. *Exerc Sport Sci Rev* **37**,
703 147-153.

704 Palmieri-Smith RM & Lepley LK (2015). Quadriceps strength asymmetry after anterior
705 cruciate ligament reconstruction alters knee joint biomechanics and functional
706 performance at time of return to activity. *Am J Sports Med* **43,** 1662–1669.

707 Palmieri-Smith RM, Thomas AC & Wojtys EM (2008). Maximizing Quadriceps
708 Strength After ACL Reconstruction. *Clin Sports Med* **27,** 405–424.

709 Revill AL & Fuglevand AJ (2017). Inhibition linearizes firing rate responses in human
710 motor units: implications for the role of persistent inward currents. *J Physiol* **595,**
711 179–191.

712 Rice DA & McNair PJ (2010). Quadriceps Arthrogenic Muscle Inhibition: Neural
713 Mechanisms and Treatment Perspectives. *Semin Arthritis Rheum* **40,** 250–266.

714 Rocchi JE, Labanca L, Laudani L, Minganti C, Mariani PP & Macaluso A (2020).
715 Timing of Muscle Activation Is Altered During Single-Leg Landing Tasks After
716 Anterior Cruciate Ligament Reconstruction at the Time of Return to Sport. *Clin J*
717 *Sport Med* **30**, e186-e193.

718 Shelbourne KD & Nitz P (1992). Accelerated Rehabilitation after Anterior Cruciate
719 Ligament Reconstruction. *J Orthop Sport Phys Ther* **15,** 256–264.

720 Tegner Y & Lysholm J (1985). Tegner Score. *Clin Orthop Relat Res* **198**, 43-49.

721 Thompson CK, Negro F, Johnson MD, Holmes MR, McPherson LM, Powers RK,
722 Farina D, Heckman CJ (2018). Robust and accurate decoding of motoneuron
723 behaviour and prediction of the resulting force output. *J Physiol* **596,** 2643-2659.

Van Cutsem M, Feiereisen P, Duchateau J & Hainaut K (1997). Mechanical Properties and Behaviour of Motor Units in the Tibialis Anterior During Voluntary Contractions. *Can J Appl Physiol* **22,** 585–597.

Additional Information

Competing interests

None of the authors has any conflicts of interests.

Data Availability Statement

The data that support the findings of this study are available from the corresponding author upon reasonable request.

Funding

No funding to declare.

Acknowledgments

The authors would like to acknowledge all the volunteers who participate with entusiasm and commitment to the study.

Author Contribution

SN, ADV and AC acquired and analysed the data. SN drafted the manuscript and plotted the figures. All authors contributed to the conception of the work, revised it critically for important intellectual content, approved the final version of the manuscript and agree to be accountable for all aspects of the work. All persons designated as authors qualify for authorship, and all those who qualify for authorship are listed.